ISSN 1024-8560, Atmospheric and Oceanic Optics, 2018, Vol. 31, No. 5, pp. 471–478. © Pleiades Publishing, Ltd., 2018.
Original Russian Text © V.V. Belov, Yu.B. Burkatovskaya, N.P. Krasnenko, A.S. Rakov, D.S. Rakov, L.G. Shamanaeva, 2018, published in Optika Atmosfery i Okeana.

ACOUSTOOPTICAL AND RADIOOPTICAL METHODS FOR ENVIRONMENTAL STUDIES

Experimental and Theoretical Investigations of the Near-Ground Propagation of Acoustic Radiation in the Atmosphere

V. V. Belov[a], Yu. B. Burkatovskaya[b, c], N. P. Krasnenko[d, e, *], A. S. Rakov[d, e], D. S. Rakov[c, d], and L. G. Shamanaeva[a, b]

[a] *V.E. Zuev Institute of Atmospheric Optics, Siberian Branch, Russian Academy of Sciences, Tomsk, 634055 Russia*
[b] *Tomsk State University, Tomsk, 634050 Russia*
[c] *Tomsk Polytechnic University, Tomsk, 634050 Russia*
[d] *Institute of Monitoring of Climatic and Ecological Systems, Siberian Branch, Russian Academy of Sciences, Tomsk, 634055 Russia*
[e] *Tomsk State University of Control Systems and Radioelectronics, Tomsk, 634050 Russia*
**e-mail: krasnenko@imces.ru*

Received September 4, 2017

Abstract—Near-ground propagation of monochromatic acoustic radiation at frequencies of 300, 1000, 2000, and 3150 Hz along atmospheric paths up to 100 m long is investigated experimentally and theoretically depending on altitudes of the acoustic source and receiver. The experiment was carried out at the experimental site of the Institute of Monitoring of Climatic and Ecological Systems (IMCES) using a specially developed setup. The dependence of the recorded sound pressure level on the propagation path length and initial signal power is analyzed. The theoretical analysis is performed by the Monte Carlo method using the local estimation algorithm developed by the authors. The comparison of the experimental and theoretical results shows their satisfactory agreement, which indicates the effectiveness of the proposed algorithm and its applicability to predicting the near-ground sound propagation.

Keywords: atmospheric acoustics, near-ground propagation of acoustic radiation, Monte Carlo method, absorption, refraction, sound scattering by atmospheric turbulence

DOI: 10.1134/S1024856018050044

INTRODUCTION

The study of sound propagation in the near-ground layer of the atmosphere is of special interest for environmental acoustics. The interest is related to prediction of noise propagation in the atmosphere and the monitoring of the noise level in urban environment. Features of the near-ground propagation of acoustic waves were considered in [1, 2] where it was noted that wave characteristics are affected by many factors including the divergence of radiation from the source, state of the underlying surface and its relief, altitudes of the source and receiver, length of the propagation path, meteorological conditions, molecular and classical absorption, and refraction and scattering of sound by atmospheric turbulence, which should be taken into account in developing different prediction models. Refraction of sound is caused by gradients of the mean temperature and wind velocity. Molecular and classical absorption of sound are of exponential character and depend on air temperature and humidity. Sound scattering by fluctuations of atmospheric temperature and wind velocity, which causes additional exponential turbulent attenuation of sound and manifests itself most intensely in the surface air layer under conditions of atmospheric instability, is the least understood [3].

This work presents results both of field measurements of the intensity of sound from a powerful directed source during propagation along short near-ground paths under monitored meteorological conditions and of solutions of the problem of acoustic radiation propagation by the Monte Carlo method. The dependence of the received signal intensity on the sound wavelength, altitudes of the sound source and receiver, propagation path length, outer scale of atmospheric turbulence, and albedo of the underlying surface is studied. The theoretical results are compared with data of experimental studies and results of calculations using the Delany–Bazley underlying surface-impedance model.

RESULTS OF THE EXPERIMENTAL STUDIES

Field experiments on the sound signal propagation over a solid homogenous underlying surface with herbaceous cover were carried out on a path with a length

Fig. 1. Exterior view of the 91-element antenna array.

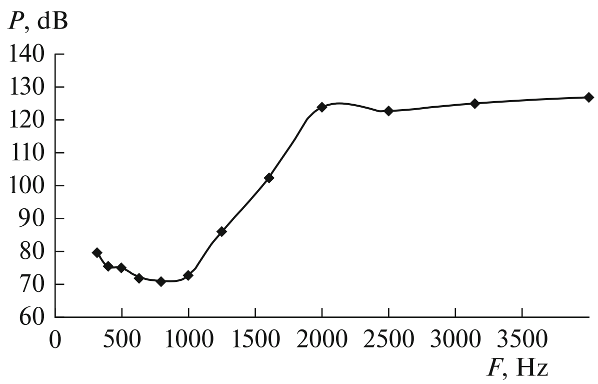

Fig. 2. Amplitude-frequency characteristic of the antenna array at a distance of 20 m from the source.

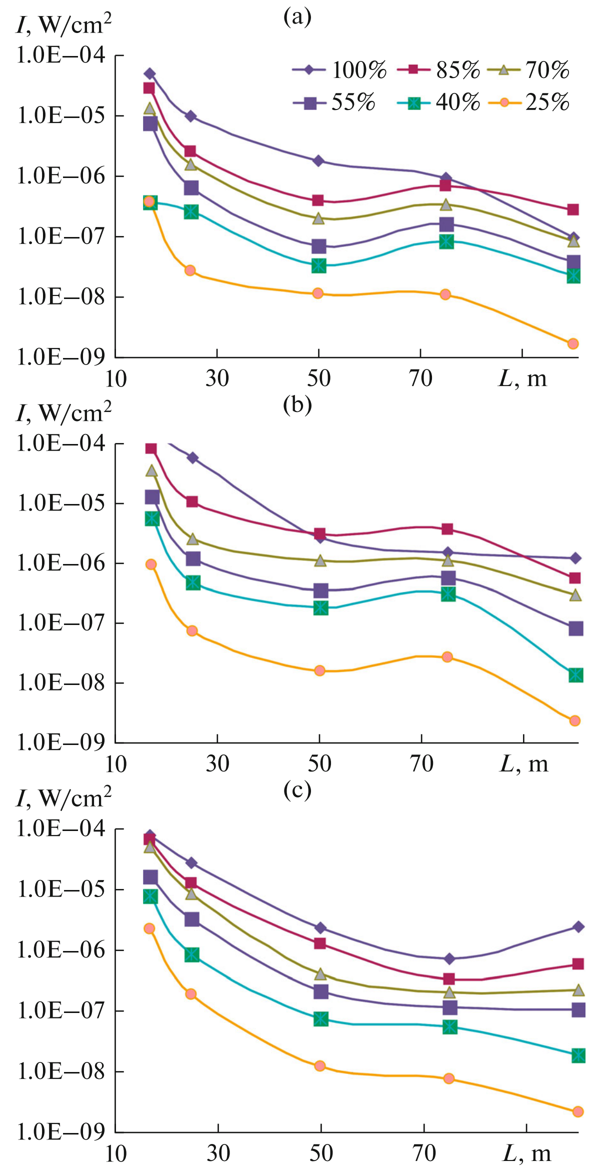

Fig. 3. Sound intensity I as a function of the distance L from the receiver for sound frequencies F = (a) 3150, (b) 2500, and (c) 2000 Hz and sound source power, as a percentage of the maximum value P_s = 152 (3150 Hz), 147 (2500 Hz), and 142 dB/m (2000 Hz).

of up to 100 m on a specially developed facility on the IMCES experimental site. A powerful acoustic antenna array [4] with generated sound pressure of up to 155 dB/m was used as an acoustic radiation source. The exterior view of the array is shown in Fig. 1; its amplitude-frequency characteristic, in Fig. 2. The source and receiver of sound were placed at an altitude of 3.5 m.

The level of sound pressure at the path was measured with an Ekofizika 110A first-order sound level meter at distances of 10, 17, 25, 50, 75, and 100 m from the source at frequencies of 2000, 2500, and 3150 Hz. The antenna beam widths relative to a level of −3 dB at frequencies of 2000, 2500, and 3150 Hz were 14°, 12°, and 10°, respectively. The air temperature was 20°C; humidity, 52%; atmospheric pressure, 747 mm Hg. The underlying surface had a herbaceous cover with a height of 0.5–0.7 m. The experimental data were processed using special software supplied with the sound level meter. In addition, standard tools of Windows and Microsoft Excel were used. The results for the sound intensity depending on the distance from the receiver are shown in Fig. 3.

Analysis of the results demonstrates that they are well approximated by a third-order polynomial

$$I(L) = AL^3 + BL^2 + CL + D. \qquad (1)$$

The approximation coefficients are shown in Table 1 for every measurement.

THEORETICAL ESTIMATES BY THE MONTE CARLO METHOD

Monte Carlo calculations involved a 500-m plane-stratified model of a turbulent atmosphere divided into 25 layers z_j, j = 1, ..., 25. Inside the layers, coeffi-

Table 1. Approximation coefficients of sound intensity in formula (1)

Source power P, dB/m	A	B	C	D
		$F = 2000$ Hz		
142	9.25×10^{-5}	-0.01	-7.89×10^{-3}	120.335
141	7.30×10^{-5}	-8.26×10^{-3}	-0.12	119.415
140	7.70×10^{-5}	-9.04×10^{-3}	-0.09	116.43
138	5.58×10^{-5}	-5.86×10^{-3}	-0.19	113
137	-2.57×10^{-6}	3.1×10^{-3}	-0.59	113
134	2.70×10^{-5}	-2.2×10^{-3}	-0.34	103
		$F = 2500$ Hz		
147	9.25×10^{-5}	-5.95×10^{-4}	-0.48	128.434
146	7.30×10^{-5}	0.02	-1.22	131.325
145	7.70×10^{-5}	0.02	-1.29	127.818
144	5.58×10^{-5}	0.03	-1.52	126.48
142	-2.57×10^{-6}	0.03	-1.61	123.017
139	2.70×10^{-5}	0.03	-1.54	114.596
		$F = 3150$ Hz		
152	-9.36×10^{-4}	0.017	-1.15	130
151	-1.93×10^{-4}	0.038	-2.38	143
150	-1.84×10^{-4}	0.036	-2.22	138
148	-1.84×10^{-4}	0.036	-2.24	134
147	-2.18×10^{-4}	0.041	-2.38	128
144	-1.93×10^{-4}	0.036	-2.11	119

cients of classical and molecular absorption ($\sigma_{\rm cl}$ and $\sigma_{\rm mol}$), coefficients of scattering by turbulent fluctuations of temperature (σ_T) and wind velocity (σ_V), and phase functions of scattering by turbulent fluctuations of temperature ($g_T(\theta)$) and wind velocity ($g_V(\theta)$) were constant [5–7]. The underlying surface was assumed to be both absolutely absorbing (radiation reflection factor (albedo) of the underlying surface $\Lambda = 0$) and absolutely reflecting ($\Lambda = 1$). The calculations were carried out for unstable atmospheric stratification in low-wind conditions. Sound absorption in the atmosphere was calculated by the method [8]. Outer scales of temperature and dynamic turbulence (L_{0T} and L_{0V}) were specified by analytical relations proposed in [9] for a cloudless (the surface heat flux $H_s = 200$ W/m^2) and cloudy atmosphere ($H_s = 40$ W/m^2). The source of continuous acoustic radiation with a given power P and divergence angle ϕ depending on the frequency was placed at the altitude $z_s = 3.5$ m above the underlying surface. The radiation receiver was also positioned at the altitude $z_r = 3.5$ m above the underlying surface.

The general scheme of the algorithm of direct statistical modeling of phonon trajectories in a turbulent atmosphere was described in [5, 6]. In this work, a modification of the Monte Carlo method for calculating local radiation characteristics at the receiver point [7] was used. According to this modification, the probability density that the given trajectory terminates at a given sth point of the space is calculated at every ith scattering point. The probability density of this event up to a constant is

$$p = \upsilon_i \exp(-\tau_{i,s}) g(\boldsymbol{\omega}_i, \boldsymbol{\omega}_s)/\rho_{i,s}^2, \quad (2)$$

where υ_i is the statistical weight of the phonon; $\rho_{i,s}$ is the geometric distance between points i and s; $\tau_{i,s}$ is the dimensionless length of the segment connecting the spatial points i and s, i.e.,

$$\tau_{i,s} = \int_{r_i}^{r_s} (\sigma_{\rm cl}(r) + \sigma_{\rm mol}(r) + \sigma_T(r) + \sigma_V(r))dr;$$

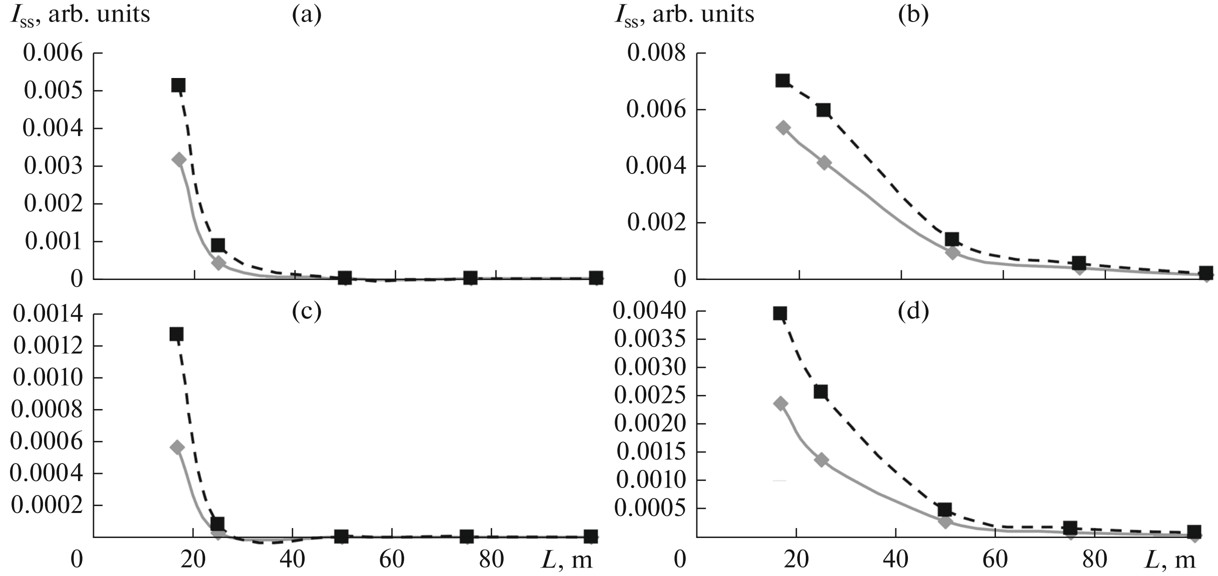

Fig. 4. Statistical estimates of acoustic radiation intensity I at frequencies of (a, b) 2000 and (c, d) 2500 Hz as functions of the propagation path length L.

and $g(\boldsymbol{\omega}_i, \boldsymbol{\omega}_s)$ is the probability density that a phonon is scattered from point i toward point s. The calculations were carried out for 10^6–10^7 phonon events, which provided the variance of the obtained results at a level of 3–10%.

Following are results of Monte Carlo calculations for the case of an absolutely absorbing underlying surface, source altitude $z_s = 3.5$ m, angle of source radiation divergence $\phi = 14°$, and receiver altitude $z_r = 3.5$ m. Figure 4 shows statistical estimates of the intensity of singly scattered (I_{ss}) and multiply scattered (I_{ms}) acoustic radiation at frequencies of 2000 and 2500 Hz depending on the propagation path length L under conditions of low wind $V = 1$ m/s and unstable cloudless (dashed curves) and cloudy atmosphere with weak turbulence and stratification close to neutral (solid curves). It follows from the comparison of the curves that atmospheric turbulence has a significant effect on the process of sound propagation in the near-ground atmosphere.

It is seen that multiple scattering makes the main contribution to the radiation detected by the device. Besides, it attenuates with distance more slowly than the singly scattered radiation. The influence of meteorological conditions is also clearly discernible. At 2000 Hz, the radiation intensity decreases approximately by five times with an increase in the length of the propagation path from 17 to 50 m; at 2500 Hz, it decreases approximately by eight times.

The effect of the receiver altitude z_r and albedo of the underlying surface on the power of the received signal is illustrated by Fig. 5.

It is seen that the received power of the signal increases with the albedo of the underlying surface. For example, at 1000 Hz, it increases by factors of 1.65, 1.69, and 2.1 at $z_r = 0$, 0.5, and 1 m, respectively; at 2000 Hz, it increases by as much as factors of 3.1, 5, and 3.4 for the same values of the receiver altitude.

The Monte Carlo method allows one to estimate the effect of individual factors of a multifactor process. In our case, estimates show a significant (up to five times) effect of the underlying surface on the acoustic signal power during propagation along surface paths, as well as the enhancement of the effect of the surface albedo with an increase in the sound frequency. An increase in the source altitude of 1 m leads to an increase in the received power of the signal by factors of 1.3 and 1.7 for $\Lambda = 0$ and 1 and $F = 1000$ Hz; the power of the received signal at 2000 Hz for $\Lambda = 0$ and $z_r = 0$ increases by a factor of 2.8; for $\Lambda = 1$ and $z_r = 1$ m, it decreases by a factor of 0.9, which can be explained by the interference of the direct and reflected waves.

COMPARISON OF EXPERIMENTAL AND THEORETICAL RESULTS

In the course of calculations, the initial data corresponded to field experiments on propagation of sound waves over the underlying surface. For example, Fig. 6 shows results of experimental measurements on June 7, 2007, for the following parameters: antenna beam widths relative to a level of −3 dB at frequencies of 2000, 2500, and 3150 Hz were 14°, 12°, and 10°, respectively; the air temperature was 10.4°C; humidity, 97%; atmospheric pressure, 1009.3 hPa; the

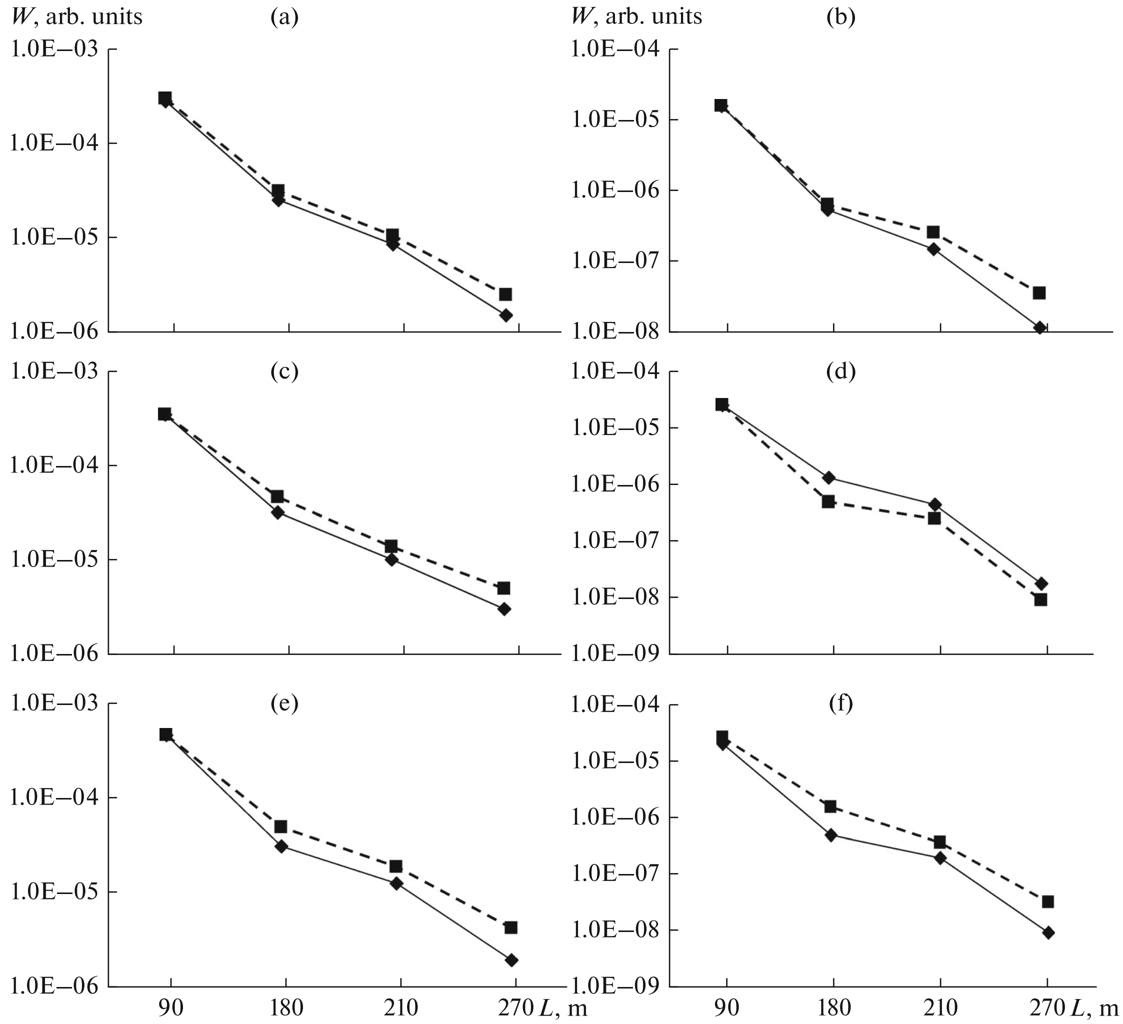

Fig. 5. Theoretical dependence of the received acoustic signal power W on the propagation path length L for sound frequencies F = (a, c, e) 1000 and (b, d, f) 2000 Hz; the receiver altitude z_r = (a, b) 0, (c, d) 0.5, and (e, f) 1 m; for an absolutely absorbing ($\Lambda = 0$) (solid curve) and absolutely reflecting surfaces ($\Lambda = 1$) (dashed curve). The source altitude z_s = 6 m, the radiation divergence angle $\phi = 5°$, and the Monin–Obukhov length scale $L_{MO} = -2.4$ m.

underlying surface had an herbaceous cover with a height of 0.5–0.7 m. The receiver altitude is shown in the figure.

Results of calculations with the same values of the parameters are presented in Fig. 7. It is seen from the comparison of experimental and theoretical results that the calculated data well reproduce experimental ones. For example, Figs. 6a and 7a show that the sound pressure level for a frequency of 300 Hz first increases with the distance, reaches the maximum at 180 m, and then decreases. For higher frequencies, the sound pressure level monotonically decreases both in the experiment (Figs. 6b–6d) and by theoretical estimates (Figs. 7c–7f). With an increase in the receiver altitude, the sound pressure level increases in both cases.

Figure 8 presents results of the comparison of experimental (curves *1* and *2*) and calculated estimates of the fraction of transmitted radiation (curves *3* and *4* with allowance for the contribution of multiple scattering) for three sound frequencies F = (a): 2000, 2500, and 3150 Hz. The experiment demonstrates a stronger decrease in the fraction of the transmitted radiation with an increase in the frequency. The difference between the experimental and theoretical data decreases with an increase in L and sound frequency: the theoretical and experimental estimates almost coincide for F = 2500 and 3150 Hz for L = 75 and 100 m, which corroborates the effectiveness of our algorithm.

Figure 9 presents the experimental dependence (dashed curves) of P for these sound frequencies on L and results of analytical calculations (solid curves) for an underlying surface with impedance specified by the Delany–Bazley model [2, 10].

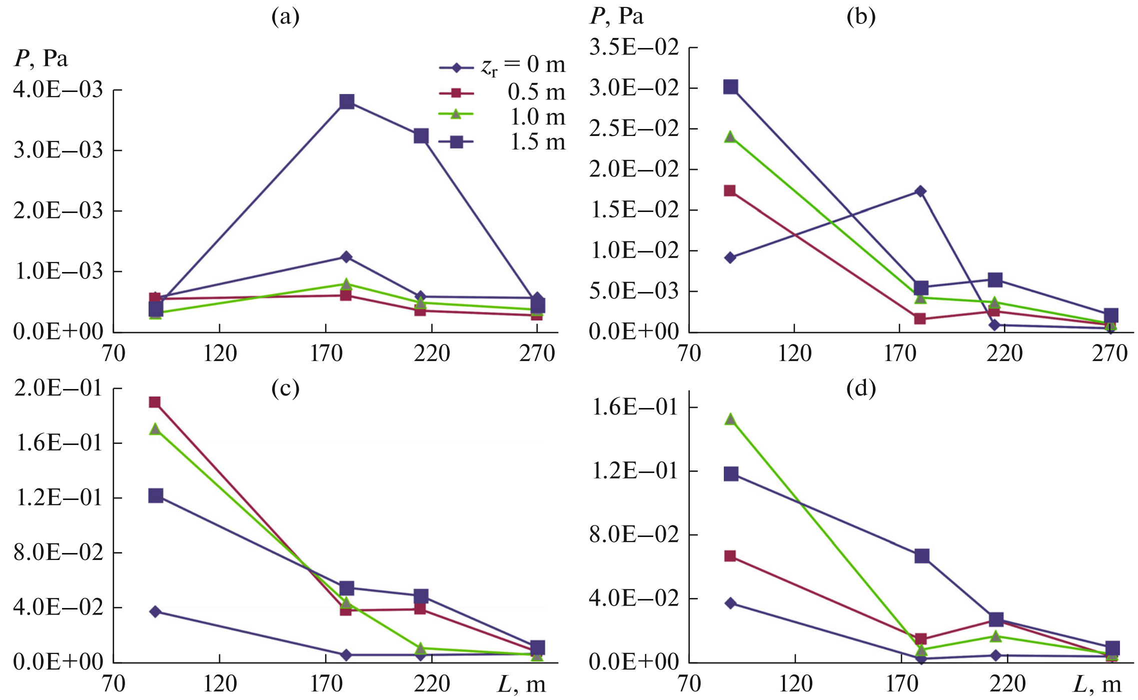

Fig. 6. Experimental dependence of the level of sound pressure P on propagation path length L for sound frequencies of (a) 315, (b) 1000, (c) 2000, (d) 3150 Hz, and different receiver altitude.

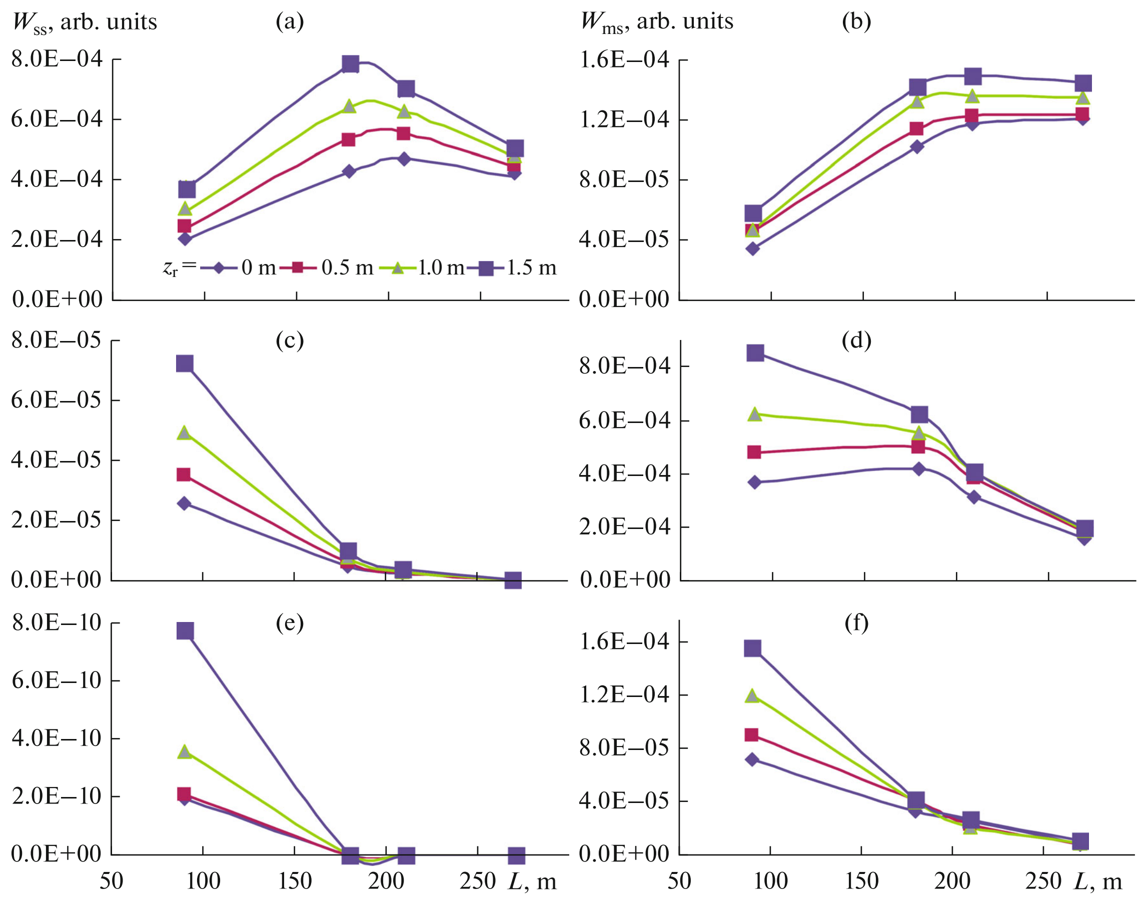

Fig. 7. Theoretical estimates of the sound pressure level for a single scattered W_{ss} and multiply scattered W_{ms} sound signal according to the Monte Carlo method for the same values of meteorological parameters and receiver altitudes as in the experiment in Fig. 6 and sound frequencies of (a, b) 300, (c, d) 1000, and (e, f) 2000 Hz.

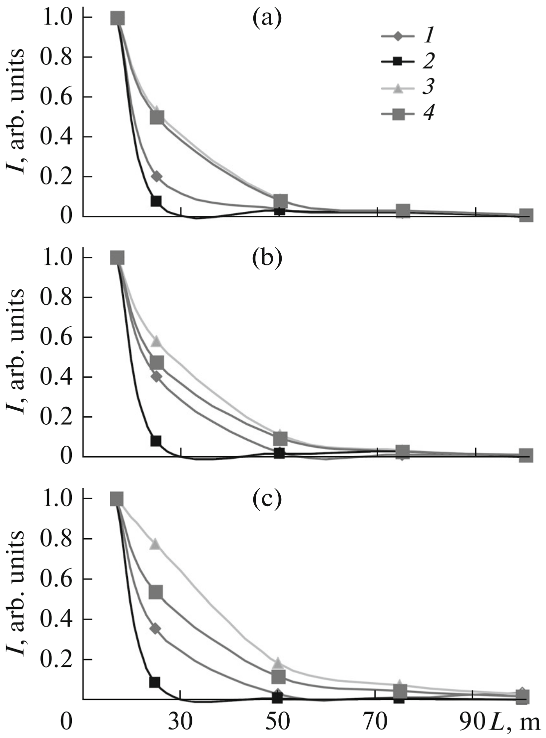

Fig. 8. Experimental and theoretical estimates of the fraction of transmitted radiation for sound frequencies of (a) 2000, (b) 2500, and (c) 3150 Hz; maximal (*1*) and minimal (*2*) transducer power in the experiment; total sound attenuation at the minimal (*3*) and maximal (*4*) power of the transducer according to the Monte Carlo calculations.

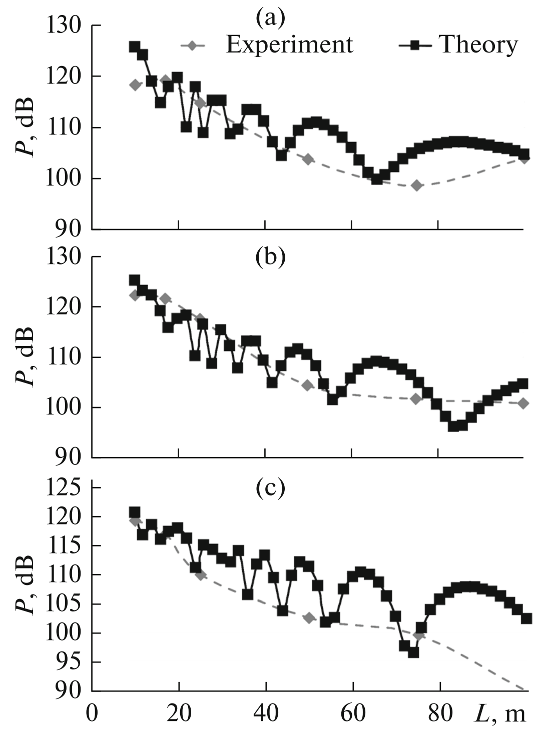

Fig. 9. Experimental dependence of sound pressure (dashed curves) during the propagation of acoustic radiation at frequencies of (a) 2000, (b) 2500, and (c) 3150 Hz over the underlying surface on the propagation path length (the source and receiver altitudes $z_s = z_r = 3.5$ m). Results of analytical calculations using the Delany–Bazley impedance model (solid curves).

According to Fig. 9, results of the theoretical calculation of near-ground sound propagation with the use of the Delany–Bazley impedance model correlate well and adequately coincide with experimental data.

CONCLUSIONS

In this work, the problem of the monochromatic acoustic radiation propagation along a near-ground path has been solved by the Monte Carlo method with allowance for the contribution of multiple scattering, sound refraction, and reflection by the ground surface for the cloudy and cloudless models of the atmosphere depending on the propagation path length for sound frequencies of 2000 and 2500 Hz and fixed altitudes of the source and receiver. It has been shown that multiple scattering of sound makes the main contribution to the radiation detected by the device. Besides, multiply scattered radiation attenuates with the distance more slowly than singly scattered radiation. At a frequency of 2000 Hz, the radiation intensity decreases approximately by five times as the length of the propagation path increases from 17 to 50 m; at a frequency of 2500 Hz, approximately by eight times. The effect of meteorological conditions is tracked. The data of field measurements of sound pressure have been presented. They have been compared with results of the analytical calculation for an underlying surface the impedance of which was specified by the Delany–Bazley model. The comparison shows a satisfactory agreement. For statistical estimations, conditions of field experiments on the propagation of sound waves over the underlying surface were taken as initial parameters.

ACKNOWLEDGMENTS

This work was supported in part by the Ministry of Education and Science of the Russian Federation (project no. 5.3279.2017/4.6) and the Russian Foundation for Basic Research (project no. 16-01-00121a). Results of simulation were obtained within the framework of the Tomsk Polytechnic University Competitiveness Enhancement Program.

REFERENCES

1. E. M. Salomons, *Computational Atmospheric Acoustics* (Kluwer Academic Publishers, Dordrecht, Boston, London, 2001).
2. K. Attenborough, K. M. Li, and K. Horoshenkov, *Predicting Outdoor Sound* (Taylor & Francis, London, New York, 2007).

3. D. K. Wilson, C. L. Pettit, and V. E. Ostashev, "Sound propagation in the atmospheric boundary layer," Acoust. Today **11** (2), 44–53 (2015).

4. N. P. Krasnenko, A. N. Kudryavtsev, A. S. Rakov, and D. S. Rakov, "Investigation of the characteristics of a high-power transmitting acoustic antenna array," Dokl. TUSUR, No. 4 **38**, 47–51 (2015).

5. V. V. Belov, Yu. B. Burkatovskaya, N. P. Krasnenko, and L. G. Shamanaeva, "Monte Carlo method in atmospheric acoustics," Opt. Atmos. Okeana **24** (12), 1072–1077 (2011).

6. L. G. Shamanaeva, V. V. Belov, Yu. B. Burkatovskaya, and N. P. Krasnenko, "Statistical simulation of acoustic radiation propagation in the lower atmosphere by the Monte Carlo method," Proc. SPIE **8696**, 86960 (2012).

7. L. G. Shamanaeva, V. V. Belov, Yu. B. Burkatovskaya, N. P. Krasnenko, and M. V. Tarasenkov, Certificate of the State Registration of Software no. 2016619427 of August 18, 2016.

8. *Method for calculation of the absorption of sound by the atmosphere, ANSI S1.*26-1995 (American National Standard Institute, New York, 1995).

9. V. E. Ostashev and D. K. Wilson, "Relative contributions from temperature and wind velocity fluctuations to the statistical moments of a sound field in a turbulent atmosphere," Acta Acust. Acust. **86** (2), 260–268 (2000).

10. N. P. Krasnenko, A. S. Rakov, D. S. Rakov, and L. G. Shamanaeva, "Influence of Impedance Properties of the earth's Surface on Sound Attenuation During Near-Ground Propagation," Rus. Phys. J. **57** (1), 100–109 (2014).

Translated by A. Nikol'skii